

Optimal Electrode Design for In Plane Switching (IPS) Cell

Seung Su Yang, Soon Yeol Park and Teayoung Won

Department of Electrical Engineering, College of IT Engineering, Inha University
 253 Yong Hyun Dong, Nam Ku, Incheon, Korea
 TEL:82-32-875-7436, e-mail: yss@hse.inha.ac.kr.

Keywords : IPS, in-plane switching, liquid crystal display, FEM, simulation

Abstract

In this paper, we propose a novel electrode structure for In Plane Switching (IPS) mode LC cell which provides the enhanced transmittance and wider viewing angle as well as less color shift. The simulation results revealed that transmission increases by more than 11.9% and shows less color shift than the conventional S-IPS mode.

1. Introduction

Many research efforts have been made further to improve the display performance of the Liquid crystal displays (LCDs) such as the light transmittance, contrast ration, and viewing angle. Recently, the in-plane-switching (IPS) mode has attracted a great deal of attention since the in-plane molecular response to the electric field switching under the electrode architecture helps to achieve wide-viewing angle characteristics [1]. The in-plane electric field produced in the IPS cell twists the LC directors and the light from the back light unit transmits through the crossed polarizer.

The super in-plane-switching (S-IPS) mode cell, which is further an evolved version of the IPS family, comprises a couple of domains one of which is for the purpose of achieving a wide viewing angle and the other of which is for the purpose of reducing the color gamut [2]. However, the traditional IPS modes inevitably suffer from the poor light transmission as well as the huge color shift problem since quite a strong vertical electric field exists over the electrode surface [3, 4].

Therefore, we have undertaken a numerical study in an effort to devise a novel electrode architecture which ensures a superior light transmittance with less color shift as well as wide viewing angle characteristics. Our numerical study consists of the investigation of the molecular behavior of liquid crystals and the consequent electro-optic properties as a light-valve with a finite element method (FEM)

numerical software, 'TechWiz LCD', wherein the numerical engine is based on the solution of Eriksen-Leslie equations and 2×2 Jones matrix scheme for the optical analysis [5].

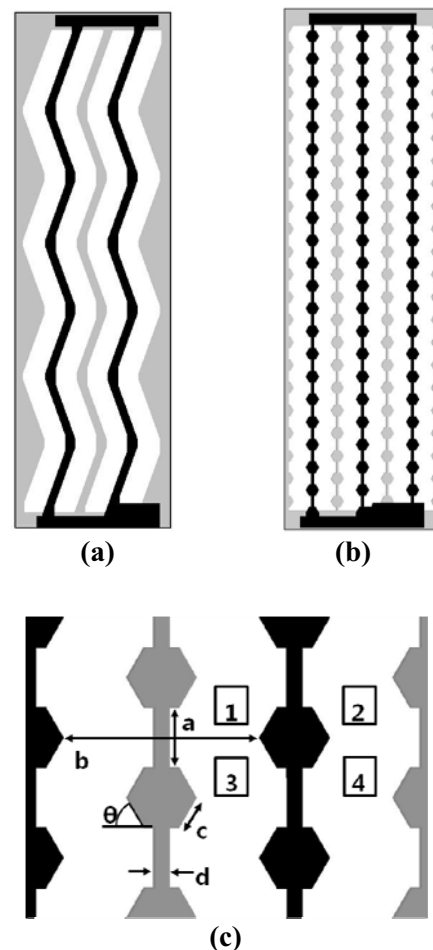


Fig.1. (a) Electrode layout of the conventional S-IPS cell. (b) Electrode layout of the proposed IPS mode cell. (c) Illustration of proposed electrode structure in detail.

2. Device Design and Simulation Parameters

Figures 1(a) and 1(b) are schematic diagrams illustrating the architectures of the common and pixel electrodes for the prior-art reference IPS and our novel IPS mode, respectively. We employed the super IPS mode as the reference. We assumed the transparent metal (ITO) for pixel and common electrodes wherein they are separately deposited on the same substrate. The simulation window is assumed to be $70 \mu\text{m} \times 234 \mu\text{m}$ while the sizes of pixel electrode and common electrode for the reference S-IPS are $56 \mu\text{m} \times 231 \mu\text{m}$ and $88 \mu\text{m} \times 234 \mu\text{m}$, respectively. The sizes of the pixel electrode and common electrode for the proposed IPS architecture is $69.6 \mu\text{m} \times 219.3 \mu\text{m}$ and $70 \mu\text{m} \times 222.8 \mu\text{m}$, respectively.

Figure 1(c) is a layout which illustrates the proposed hexagonal electrode architecture for the IPS mode operation which has been thoroughly investigated and optimized in this work. The proposed IPS electrode structure has a feature in that the pixel electrode as well as the common electrode has a hexagonal shape. Furthermore, the individual hexagonal electrode is connected to each other through the main bone electrodes. The distance between the two neighboring hexagons, which is denoted as “a”, has been optimized as $5 \mu\text{m}$ while the distance “b” is $16.5 \mu\text{m}$. The hexagons are of regular shape and have a side length, which is denoted as “c”, of $3 \mu\text{m}$ and the tilt angle of the hexagon edge, which is denoted as “ Θ ”, of 60° . The width of the main bone electrodes, which is denoted as “d”, is $1.5 \mu\text{m}$.

Table 1 illustrates the simulation condition which has been employed in this simulation study. We assumed the common electrode is tied to the ground potential. As an LC material, a positive $\Delta\epsilon$ LC material MLC-6692 with $K_{11}=9.2 \text{ pN}$, $K_{22}=6.1 \text{ pN}$, $K_{33}=14.6 \text{ pN}$, $\Delta\epsilon=10.3$, $n_o=1.4771$ and $n_e=1.5621$ at $\lambda=589 \text{ nm}$ is used, wherein the cell gap is $4.4 \mu\text{m}$ and pre-tilt angle is 2° and the initial azimuthal angle (i.e. the rubbing angle) is 90° . When there is no voltage applied, the incident light is completely blocked by the cross polarizer, which results in a normally black state. When the applied voltage exceeds the threshold, the transversal electric fields are created and the electric field lines are in the parabolic form in the whole display area.

TABLE 1. Parameters used in the simulation cells.

LC	MLC-6692
Rubbing angle	90
Pre-tilt angle	2
Cell gap	$4.4 \mu\text{m}$
a	$11.2 \mu\text{m}$
b	$16.5 \mu\text{m}$
c	$3 \mu\text{m}$
θ	60°
Simulation size	$70 \mu\text{m} \times 234.1 \mu\text{m}$

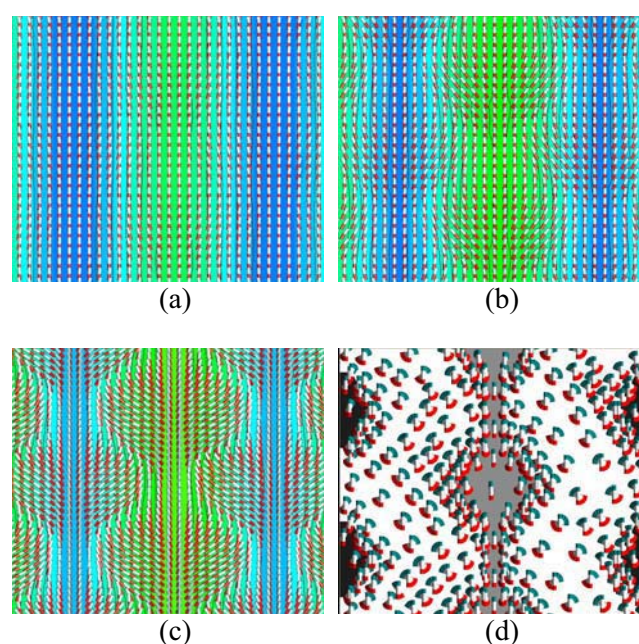


Fig. 2 Director distribution in the middle of the liquid crystal layer, (a) 5V, (b) 6V, (c) 7V. (d) Top view of the director distribution on the liquid crystal layer when 7V is applied.

3. Simulation Results and Discussion

Figure 2 is a plot which illustrates the electric potential contours and the LC director distributions of our novel IPS cell. Referring to Figure 2, we can see the orientation of the director as well as the potential distribution at the middle of the liquid crystal layer. Figures 2(a), 2(b) and 2(c) provide the director distributions at a xy-plane under the voltages of 5V, 6V and 7V, respectively. In Figures 2(a), 2(b), and 2(c), we should note that the background color indicates the potential distribution. The rotation of the cylinder symbols indicates the angle of local twist while the length of the symbols indicates the

magnitude of the tilt angle. The color of the cylinder symbols indicates the direction of the twisted director.

Figure 2(d) is a top view of the simulated LC director distribution at the liquid crystal layer when 7V is applied. When the applied voltage goes beyond the threshold, the LC molecules in the regions 1 and 4 tend to rotate in a clockwise direction while those in the regions 2 and 3 start to rotate in a counterclockwise direction. This counter rotation of directors in both regions is considered to be very effective for compensating the color shift [6, 7].

Figure 3 is a diagram illustrating the light transmittance as a function of the applied voltage for the conventional S-IPS and the proposed IPS mode cell. Total amount of calculated transmittance of the proposed IPS cell with hexagonal electrode is found to be approximately 11.9% higher than that of the conventional S-IPS when 7V is applied.

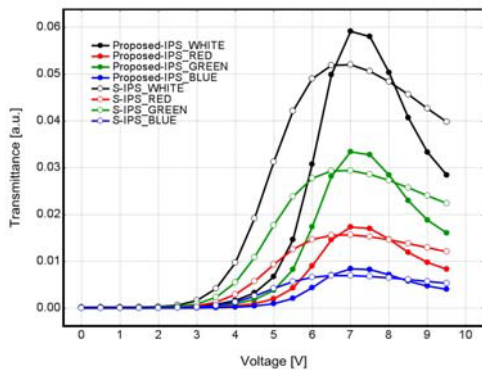


Fig.3. Voltage-dependent light transmittance curves for the conventional Super-IPS and the proposed IPS mode.

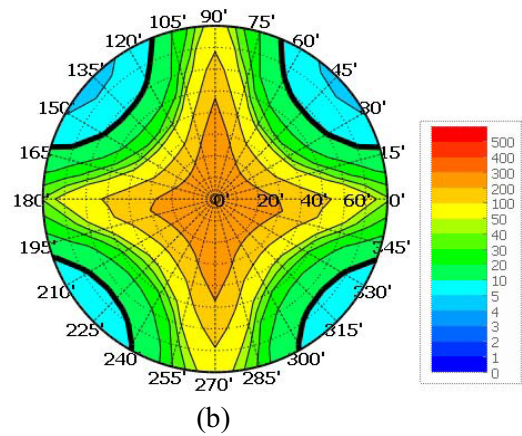
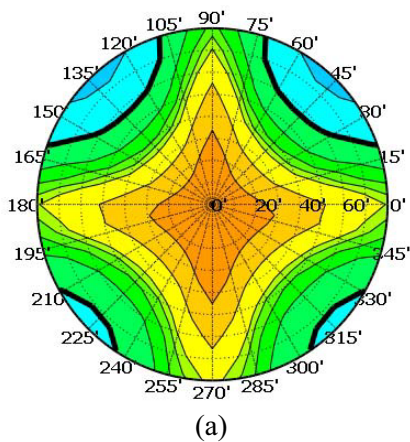


Fig.4. ISO-Contrast plot for (a) the S-IPS cell and (b) the proposed IPS cell.

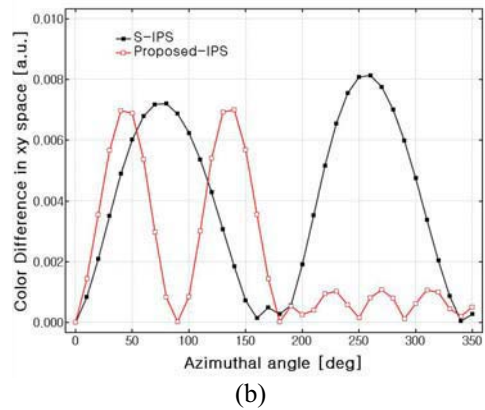
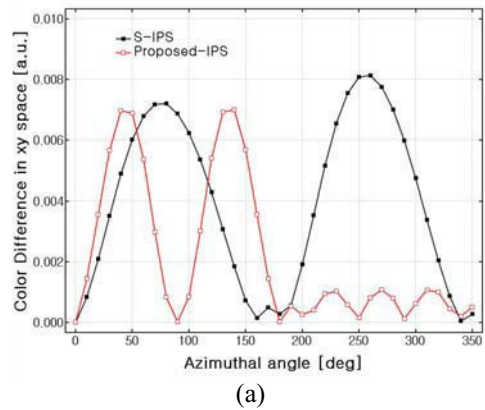


Fig.5. Dependence of color shift on viewing direction. (a) Dependence on the azimuth angle. (b) Dependence of color shift on viewing angle.

Figure 4 is a polar plot which illustrates the iso-contrast ratio (CR) contours of S-IPS and proposed novel electrode IPS mode cell, respectively, under their respective maximum transmittance voltages at a

wavelength $\lambda=589$ nm. The black line in each polar chart represents the contrast ratio wherein the value of CR is set 10. Even without the use of the compensation films, the viewing angle for $CR \geq 10:1$ has been found to improve when we compare the proposed IPS mode cell with the conventional S-IPS.

Referring to Figure 4(b), we can see that the proposed IPS structure exhibits a 350:1 contrast ratio at the volume which is defined by the $\pm 30^\circ$ view cone, and 10:1 at the volume which is defined by the $\pm 70^\circ$ view cone. In the meanwhile, the reference S-IPS exhibits a 300:1 contrast ratio at the volume which is defined by the $\pm 20^\circ$ view cone and 10:1 CR at the volume which is defined by the $\pm 60^\circ$ view cone. Therefore, the simulation study implies that the proposed novel hexagonal IPS mode exhibits the wider viewing angle characteristics over the conventional S-IPS even without using any compensation films.

Figure 5 is a schematic diagram which illustrates the color difference as a function of azimuth angle for the reference S-IPS mode cell and the proposed hexagonal electrode structure IPS mode cell, respectively. The calculated color difference is plotted in 1976 CIE coordinates wherein azimuth and polar dependence of color difference are illustrated. Referring to Figures 5(a) and 5(b), we can recognize that the hexagonal electrode IPS mode exhibits the superior color shift performance over to the conventional S-IPS mode cell.

4. Summary

We propose a novel hexagonal IPS cell architecture which provides the wider viewing angle characteristics as well as the higher light transmittance in comparison to the traditional IPS cell. We looked into the electro-optical characteristics of the proposed architecture in detail including the voltage-transmittance (V-T) curve, contrast ratio (CR) for the optimal operation of the IPS cell. The transmittance of the proposed IPS cell is considered to be enhanced by 11.9% over the traditional S-IPS cell. Furthermore, the proposed IPS mode cell exhibits the wider viewing angle performance as well as less color shift when we compare with the traditional S-IPS architecture.

5. Acknowledgment

This research was supported by the Ministry of Knowledge Economy, Korea, under the ITRC (Information Technology Research Center) support program supervised by the IITA (Institute of Information Technology Advancement) (IITA-2008-C109008010030).

6. References

1. R.A.Soref, J. Appl. Phys., vol.45, pp. 5466–5468, (1974).
2. M.Ohe and K. Kondo, Appl. Phys. Lett., vol. 67, pp. 3895–3897, (1995.)
3. M. Schadt and W. Helfrich, Appl. Phys. Lett., vol. 18, pp. 127–128, (1971).
4. S. H. Yoon, S.I. Yoon, C.S. Lee, H.J. Yoon, M.W. Choi, J.W. Kim, T. Won, IDW'03 Proceedings, pp. 49-52, (2003).
5. H. J. Youn, C.S. Lee, M.S. Jung, S.H. Yoon, T. Won, IMID'05 Digest, pp. 515-518, (2005).
6. W. J. Shin, S.Y. Cho, J. B. Lee, H.Y. Yoon, S.H. Yoon, T. Won, AM-FPD'07 Digest, pp. 41-44, (2007).
7. S. T Wu and U. Efron, Appl. Phys. Lett., 48, 624, (1986).